A Magnetization-Transfer Nuclear Magnetic Resonance Study of the Folding of Staphylococcal Nuclease†

Philip A. Evans,‡,⊥ Roger A. Kautz,§ Robert O. Fox,§,∥ and Christopher M. Dobson*,‡

Inorganic Chemistry Laboratory, University of Oxford, South Parks Road, Oxford OX1 3QR, U.K., and Department of Molecular Biophysics and Biochemistry and The Howard Hughes Medical Institute, Yale University, New Haven, Connecticut 06520

Received March 30, 1988; Revised Manuscript Received July 7, 1988

ABSTRACT: The equilibrium between alternative folded states of a globular protein, staphylococcal nuclease, has been investigated by using ^{1}H NMR. Magnetization-transfer experiments have revealed the existence of a related structural heterogeneity of the unfolded state, and quantitative analysis of a series of these experiments has permitted the kinetics of folding and interconversion of the different states to be explored. A model based on cis/trans isomerism at the peptide bond preceding Pro-117 has been developed to account for the results. This model, recently supported by a protein-engineering experiment [Evans et al. (1987) *Nature (London) 329*, 266], has been used to interpret the kinetic data, providing insight into the nature of the folding processes. The predominance of the *cis*-proline form in the folded state is shown to derive from a large favorable enthalpy term resulting from more effective overall folding interactions. The kinetics of folding and isomerization are shown to occur on similar time scales, such that more than one pathway between two states may be significant. It has been possible, however, to compare the direct folding and unfolding rates within the *cis*- and *trans*-proline-containing populations, with results suggesting that the specific stabilization of the cis peptide bond is effective only at a late stage in the folding process.

Staphylococcal nuclease is a small, globular protein that has been extensively studied in the context of the protein folding problem. Numerous experimental approaches have been used to investigate the reversible unfolding of the protein in its thermodynamic, kinetic, and structural aspects (Anfinsen, 1975; Tucker et al., 1979a). The advent of protein engineering has brought renewed vigor to these studies (Shortle, 1986; Evans et al., 1987). However, a detailed understanding of the sequence of structural events that constitute the folding and unfolding processes remains, as yet, elusive. Recently, an interesting new dimension to the problem has been revealed by NMR spectroscopy (Fox et al., 1986) because two distinct folded forms of nuclease were shown to coexist at equilibrium. Although apparently closely similar in structure, these species were shown to interconvert only slowly in solution. Preliminary studies of their folding and interconversion kinetics were undertaken, and evidence was found for a related heterogeneity of the unfolded state. On the basis of these results it was suggested that isomerism about a single X–proline peptide bond might underlie the conformational differences. Subsequently, a mutant nuclease was constructed in which one of the proline residues, Pro-117, had been replaced by glycine. This protein did not exhibit alternative folded states, and this was taken to support strongly the proposal that cis/trans isomerism about the Lys-116/Pro-117 peptide bond gives rise to the alternative forms of the wild-type protein (Evans et al., 1987).

In this paper we report a detailed characterization of the folding and interconversion of the alternative folded species. This has been achieved through the application of magnetization-transfer (MT) techniques. These experiments have long been applied to the study of slow exchange processes in chemistry (Forsen & Hoffman, 1963; Campbell et al., 1978) and have recently been shown to be capable of yielding both qualitative and quantitative information about the reversible unfolding of proteins at equilibrium (Dobson et al., 1984; Dobson & Evans, 1984; Fox et al., 1986). In the present study, one- and two-dimensional MT experiments have been used to define qualitatively the folding equilibria, and a series of single and double saturation transfer experiments has then been analyzed in order to determine the rates of individual interconversion processes in the multisite system. We have then sought to interpret the data in terms of the proline isomerism model, taking advantage of the existence of the two folded forms to consider the effect of a specific structural perturbation on the kinetics and thermodynamics of folding.

Experimental Procedures

Staphylococcal nuclease A was produced by using a recombinant expression system in *Escherichia coli*. The initial expression vector, pBF2, was constructed by insertion of the nuclease encoding sequence downstream of the λpL promotor in the vector pAS1 (Rosenberg et al., 1983; R. A. Kautz and R. O. Fox, unpublished results). In our initial studies, a construct was employed that encoded an additional six amino acids ahead of the N-terminal residue of mature nuclease. This recombinant product has been designated nuclease R. Later, this additional sequence was deleted, to produce the expression vector pSNS1, so that the protein product was identical with that produced in *Staphylococcus aureus* except for the possibility (not yet investigated) of an N-terminal methionine residue (R. A. Kautz and R. O. Fox, unpublished results). Comparison of NMR spectra strongly suggested that the additional residues of the longer nuclease R protein are dis-

† This work was been supported by grants from the U.K. Science & Engineering Research Council (to C.M.D. and P.A.E.) and NIH (Grant AI-23923, to R.O.F.). The Stanford University NMR instrument was obtained through a shared equipment grant from NIH and NSF. C.M.D. is a member of the Oxford Enzyme Group.

‡ University of Oxford.

⊥ Present address: Department of Biochemistry, Cambridge University, Tennis Court Road, Cambridge CB2 1QW, U.K.

§ Department of Molecular Biophysics and Biochemistry, Yale University.

∥ The Howard Hughes Medical Institute, Yale University.

0006-2960/89/0428-0362$01.50/0

ordered in solution and have no discernible effect on the remainder of the molecule. All the experiments described in the present paper used the shorter nuclease A form.

The nuclease protein was prepared by growth of *E. coli* strain AR120 containing the pSNS1 plasmid in 12 L of 2× YT media (Maniatis et al., 1982) at 37 °C with aeration and stirring in a New Brunswick fermentor. The nuclease gene was induced by addition of 480 mg of nalidixic acid when the culture reached a density of OD_{600} = 0.8. The culture was maintained for an additional 3–4 h. Cells were harvested in a Sorvall continuous flow rotor and frozen at −20 °C. The cell pellet was thawed in 10 mM ammonium acetate, pH 6.0, and passed through a French press. Cell debris was removed by centrifugation at 20000*g*, and the supernatant, diluted with an equal volume of 0.6 M ammonium acetate, pH 6.0, was applied to a phosphocellulose column (Cellex P, Bio-Rad). The column was eluted with a 1:1 gradient of 0.3 M ammonium acetate, pH 6.0, and 1.0 M ammonium acetate, pH 8.0 (Moravek et al., 1969). Column fractions containing nuclease were pooled and passed over a DEAE column to remove nucleic acids that copurified with nuclease. The effluent of this column was concentrated under N_2 at 60 psi in an Amicon concentrator and dialyzed twice against 4 L of 200 mM NaCl to remove the ammonium acetate buffer and twice against distilled water. Several minor contaminating proteins precipitated during dialysis and were removed by centriguation. The protein was lyophilized and stored at −20 °C.

Nuclease solutions for NMR study were routinely made up at a concentration of 4 mM in 200 mM deuteriated sodium acetate buffer, pH 5.3, except for samples used to carry out a pH titration, in which 200 mM sodium chloride solution in D_2O was employed. NMR spectra were recorded at 500 MHz on the Bruker AM 500 spectrometer of the Oxford Enzyme Group and a General Electric GN-500 spectrometer at Stanford University. Chemical exchange processes were studied by using selective single and double saturation experiments in one dimension (Fox et al., 1986) as well as two-dimensional exchange-correlated spectroscopy (Jeener et al., 1979; Boyd et al., 1986).

Saturation of a single resonance was achieved by application of a selective pulse of measured duration from the decoupler, prior to acquisition. Selectivity was carefully checked by carrying out a series of irradiations in a region of the spectrum where no resonances occur, at varying separations from a protein resonance, so that the minimum spectral separation at which spillover effects could be neglected was determined.

Saturation of two resonances was achieved by simultaneous application of a pulse from the decoupler to one peak and a DANTE pulse of the same duration to the second one. A DANTE pulse comprises a train of very short pulses from the high-power transmitter, each separated by a brief interval, τ (Morris & Freeman, 1978). This produces selective excitation at the irradiation frequency and at side bands separated by $1/\tau$. If the pulse train is sufficiently long, selective saturation is effected. The value of τ was short enough to ensure that only one position within the span of the protein spectrum was irradiated (typically $\tau = 2 \times 10^{-4}$ s). The selectivity of the DANTE pulse improves as the length of the individual component pulses is decreased. However, if they are too short, insufficient power is delivered to bring about complete saturation. Thus, it was necessary to optimize the pulse length experimentally.

Magnetization-transfer effects were detected in these experiments either directly, by measurement of intensity changes of resolved peaks, or through difference spectroscopy. The latter was achieved by performing a second experiment, in which the saturating pulses were placed in a blank region of the spectrum, and subtracting the two FIDs obtained prior to Fourier transformation.

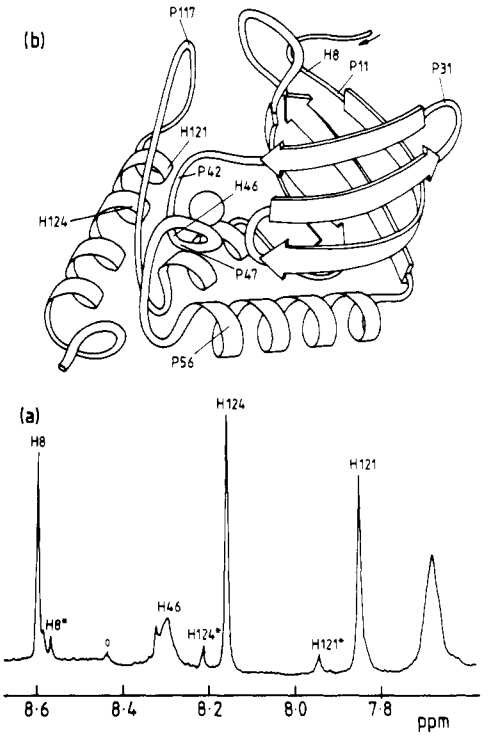

FIGURE 1: (a) Low-field region of a 500-MHz ^1H NMR spectrum of staphylococcal nuclease A, pH 5.3, 40 °C. Amide NHs have been preexchanged for deuterons, revealing the histidine $H^{\epsilon 1}$ resonances. The asterisks denote resonances of the minor folded component, designated N*. 0 denotes an impurity resonance in this and subsequent figures. (b) Schematic representation of the main-chain fold of nuclease drawn by J. S. Richardson. [Reprinted with permission from Richardson (1981). Copyright 1981 Academic Press.] The locations of the histidine and proline residues are indicated.

Two-dimensional exchange-correlated spectroscopy was carried out by using the pulse sequence $90°-t_1-90°-\tau-90°-t_2$, in which t_1 is the systematically incremented delay and t_2 the acquisition period. A mixing time, τ, of 0.45 s was employed. Phase sensitivity was achieved by the method of time proportional phase increments (Marion & Wüthrich, 1983). The time domain data comprised 512 points in the t_1 dimension and 2048 in t_2. Through zero filling and double Fourier transformation a frequency domain spectrum defined by 1024 points in ω_1 and 4096 in ω_2 was obtained.

Temperatures in NMR experiments were determined from spectra of a sample of neat ethylene glycol, calibrated against a series of melting point determinations (Evans, 1986).

Simulated NMR spectra were calculated by using the program SIMNORM, written by Dr. N. J. Clayden, implemented on a VAX 11/785 computer.

Results

Evidence for Alternative Folded Forms. The low-field region of a 500-MHz NMR spectrum of staphylococcal nuclease A is shown in Figure 1. The existence of alternative folded states is revealed by the observation of a number of minor resonances in addition to those of the major species. These are most clearly seen for the His $H^{\epsilon 1}$ resonances, as indicated in the figure. Specific resonance assignments have now been made through systematic sequence substitutions (R. A. Kautz and R. O. Fox, unpublished results; Alexandrescu et al., 1988), and these, as well as the distribution of these

Table I: Thermodynamics of Conformational and Acid–Base Equilibria for Histidine Residues of Nuclease

	[N*]/[N] at 40 °C	ΔH(N*–N) (kJ mol^{-1})	T_m (°C)	ΔH(U–N) (kJ mol^{-1})	pK_a N	pK_a N*
His-8	~0.15		48.5 ± 1		6.6	6.5
His-46			48 ± 1		5.9	
His-121	0.13 ± 0.01	45 ± 5	48.4 ± 0.4	457 ± 40	5.5	5.8
His-124	0.12 ± 0.02	42 ± 7	48.7 ± 0.5		5.9	6.0

residues in the structure, are summarized in the figure.

For three of the four histidines, His-8, -121, and -124, minor peaks can clearly be seen to accompany the major ones. In this paper we denote the major resonances H8, H121, and H124 and their corresponding minor ones H8*, H121*, and H124*. In the case of His-46 the peak is rather broad, and although an associated minor resonance has been observed under some pH and temperature conditions, this behaves quite differently from those of the other histidines. In addition, H8 appears to display a second minor resonance under certain conditions, but this behavior has yet to be fully characterized. Both of these minor peaks clearly have origins distinct from that of H8*, H121*, and H124*, which is the subject of this paper.

Examination of the temperature dependence of the nuclease spectrum revealed an entirely reversible increase in the relative intensity of the minor resonances as the temperature was raised. Above about 45 °C a thermal unfolding transition was observed, and under these conditions both major and minor forms were observed to coexist with unfolded protein, all in slow exchange on the NMR time scale. The spectral changes associated with unfolding were found to be essentially reversible, although slow irreversible changes were apparent on prolonged exposure to these conditions.

The thermodynamics of the conformational equilibria were determined by analysis of the temperature-dependent intensity changes, yielding the parameters shown in Table I. It is clear that for the two histidines followed in detail, His-121 and His-124, the equilibrium between major and minor components has the same temperature dependence, within experimental error. Qualitatively similar behavior was also confirmed for the resonances of His-8. It therefore seems most likely that the minor peaks arise not from distinct, "local", equilibria but from a common minor folded form of the protein. The major and minor components are here denoted N and N*, respectively, and the unfolded state, U.

The equilibrium between N and N* was found to be insensitive to the protein concentration in the range 0.2–6.0 mM. Similarly, it was not perturbed by urea, although this agent brought about unfolding of both components at concentrations above about 0.8 M at 32 °C. Unpublished low-angle X-ray scattering results indicate that low concentrations of urea abolish any dimer formation in nuclease solutions (J. Flanagan and D. Engelman, personal communication). All these results indicate that the alternative forms of nuclease do not result from intermolecular association.

A pH titration revealed that each minor resonance tracks its corresponding major one rather closely through the entire pH range over which the histidine H$^{\epsilon 1}$ peaks could be followed. The apparent pK_a values, shown in Table I, are within 0.1 pH unit of one another for the His-8 and His-124 pairs. In the case of His-121 the pK_a in the minor component is some 0.3 unit higher than in the major form. His-121 also differs from the others in that the chemical shifts of the two resonances cross at pH 4.8 and a separation of about 0.1 ppm persists in the low pH limit, whereas for the other histidines the chemical shifts of the two forms converge under these conditions. The general similarity of the spectra of the two components and their pH dependences suggest that the structures, in the neighborhood of these residues at least, are rather similar, the greatest disparity probably being close to His-121. These histidine residues are in quite separate regions of the folded structure (Figure 1), which indicates that the limited conformational differences between the two forms are not restricted to an isolated segment of the molecule. Further, the observation of distinct spectra of the two components indicates that there is a substantial barrier to their interconversion. Investigations were also made of the effects of ligand binding; the spectra are shown in Figure 2. Addition of Ca^{2+} affected primarily His-46, which is closest to the binding site (Markley & Jardetzky, 1970). The N/N* equilibrium was plainly unaffected, however, and elsewhere in the spectrum there was little change. When a nuclease solution with a saturating level of Ca^{2+} was titrated with a competitive inhibitor, thymidine 3′,5′-diphosphate, the minor resonances of His-8, -121, and -124 progressively diminished in intensity, reflecting a shift in the equilibrium in favor of a single conformation, close to that of N, in the ternary complex. This shows that there are sufficient differences between the two structures to cause a significant disparity in their efficacy of interaction with the nucleotide.

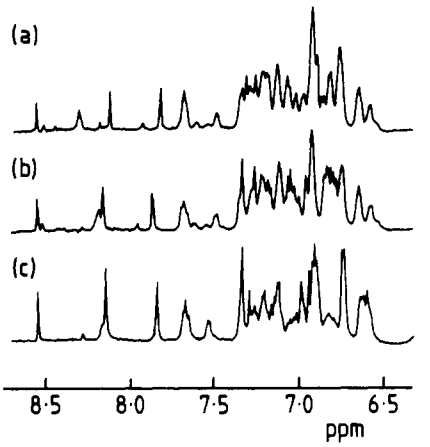

FIGURE 2: Effects of ligand binding on the ^{1}H NMR spectrum of nuclease (a) pH 5.3, 40 °C, no added ligands; (b) as in (a) but with 20 mM calcium chloride solution added; (c) as in (b) but with 7 mM thymidine 3′,5′-diphosphate.

Evidence for Alternative Unfolded Forms. Our approach to furthering understanding of the conformational multiplicity of the nuclease has been to use magnetization-transfer NMR to study the processes of interconversion of the different states under the conditions of the thermal unfolding transition.

A contour plot of part of a 2-D exchange-correlated spectrum of nuclease, close to the midpoint of unfolding, is shown in Figure 3. A number of cross-peaks are observed among the His H$^{\epsilon 1}$ resonances, which result from exchange between the different states of the protein. In the case of His-124, for example, there are cross-peaks between the resonances of the N and N* states, at 8.07 and 8.14 ppm, respectively, and also between both of these and the resonance of the unfolded state at 8.36 ppm. These demonstrate directly the interconversion of the alternative folded species with one another and with the unfolded state under these conditions. Similar patterns are observed for His-8 and His-121, except that in the latter case there is an additional cross-peak, which is discussed below. For His-46, where a resonance of the minor folded form is not resolved, there is, as expected, a single cross-peak reflecting

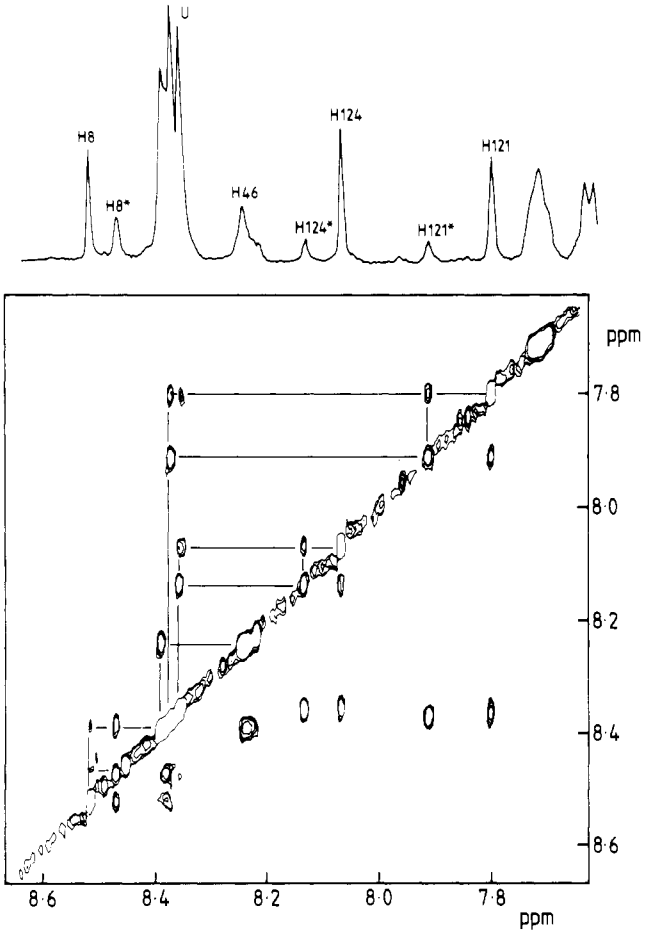

FIGURE 3: Part of a 2-D exchange-correlated spectrum of staphylcoccal nuclease recorded at 48 °C, close to the midpoint of thermal unfolding. The region of the histidine $H^{\epsilon 1}$ resonances is displayed. Experimental details are given in the text.

exchange between the folded and unfolded populations.

The major advantage of the 2-D experiment, as compared to the 1-D saturation-transfer approach, is that it does not require selective irradiation at individual frequencies, so that problems with the finite bandwidth of saturating pulses are avoided. This means that while only the resonances of His-121 are sufficiently well separated for convenient study by the 1-D MT methods, those of His-124 and His-8 were also accessible through the 2-D experiment.

It is evident in Figure 3 that the intensities of the N*/U cross-peaks are much greater than those of the N/U peaks for all three observable histidines. This would be consistent with interconversion of N* and U being much more rapid than that between N and U, as is confirmed in the 1-D experiments discussed below. The observation of the same intensity pattern for three histidines further supports the contention that these minor resonances arise from a single conformational equilibrium.

The additional remarkable effect discernible in the case of His-121 is that the major folded form gives two distinct cross-peaks with resonances of the unfolded state. These are clearly visible in the ω_2 dimension of the 2-D spectrum, although they are not resolved in the ω_1 dimension owing to lower digital resolution. This observation of two resonances of His-121 $H^{\epsilon 1}$ in the unfolded protein is amply confirmed in the 1-D experiments discussed below. The conclusion which follows is that there exist alternative unfolded, as well as folded, forms of this protein. As in the case of the folded states His-121 is the most sensitive of the four histidines to the differences between the unfolded states, since none of the

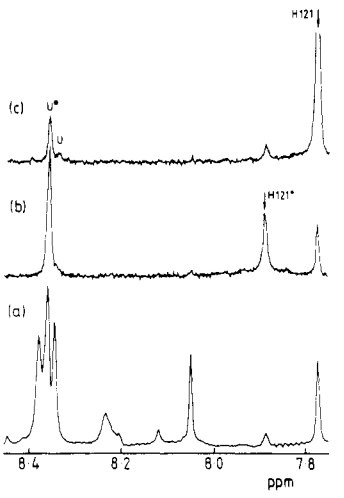

FIGURE 4: Effects of saturation of the resonances of His-121 $H^{\epsilon 1}$ in the major and minor folded states. The spectra were recorded at 48 °C, close to the midpoint of unfolding. (a) Normal spectrum; (b) MT difference spectrum, 2.5-s presaturation applied to H121*; (c) MT difference spectrum, 2.5-s presaturation applied to H121.

others gives rise to resolved twin cross-peaks in this manner. This similarity suggests that the heterogeneities of the folded and unfolded states are likely to be structurally related.

In order to estimate the relative populations of the alternative unfolded states, the cluster of histidine $H^{\epsilon 1}$ resonances arising from them in the 1-D spectrum was simulated on a computer. 1-D saturation-transfer experiments were carried out for each of the His $H^{\epsilon 1}$ folded-state peaks to determine accurately the chemical shifts and line widths of the corresponding resonances of the unfolded forms. These experiments confirmed that His-8, -46, and -124 each give rise to a single resonance on unfolding. The relative intensities of the two His-121 peaks were then varied in the simulation until the best agreement with the experimental envelope was obtained. On this basis the major unfolded form, giving rise to the more downfield of the two resonances of His-121 $H^{\epsilon 1}$, was found to constitute at least 92% of the total.

These results therefore establish the presence of four distinguishable states of the protein. In order to understand how they are interrelated, a series of 1-D single and double saturation transfer experiments was carried out. These studies were limited to His-121, since only in this case were two unfolded environments distinguished.

The effects of saturating the resonances H121 and H121* individually are compared in Figure 4. Saturation of H121 caused effects on the resonances of both unfolded species, confirming the result of the 2D experiment. When H121* was saturated, a much larger effect on the resonance of the major unfolded form was apparent, but the effect on the resonance of the minor form was actually smaller than when H121 was saturated. These observations suggest that from the major unfolded form folding to N* occurs more rapidly than to N, while the reverse is true for the minor unfolded species. In view of these relationships, which are substantiated by the detailed kinetic studies described below, the major component of the unfolded state and its His-121 $H^{\epsilon 1}$ peak will be denoted U*, while the minor component and its corresponding resonance will be denoted U.

It was pointed out under Experimental Procedures that only limited conclusions may be drawn directly from single saturation experiments in a multisite system. The effects of simultaneous saturation of both H121 and H121* were therefore investigated, as illustrated in Figure 5. It is clear that with H121* saturated, increased MT from both U* and U was

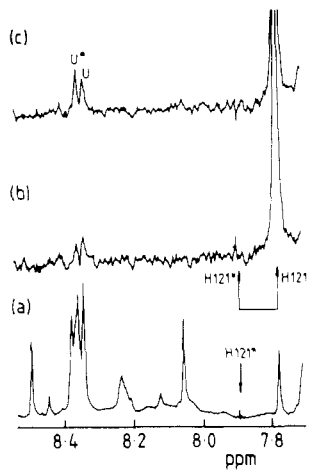

FIGURE 5: Double saturation experiment to explore the time development of magnetization transfer between H121 and U,U*. (a) Spectrum at 48 °C in which H121* had been presaturated for 3 s. (b) Difference from (a) of a spectrum in which H121 had been additionally saturated during the last 400 ms of the 3-s irradiation of H121*. (c) Difference from (a) of a spectrum in which H121 and H121* had both been saturated for a full 3 s prior to acquisition.

observed on additional saturation of H121. Since this magnetization cannot have been relayed via H121*, this shows that interconversion pathways exist between N and the two unfolded forms that do not pass through N* (Fox et al., 1986), thus showing that N* is not actually obligatory as an intermediate in the folding of N from either unfolded form.

Figure 5 shows the time dependence of MT when H121 is saturated under conditions of equilibrium MT from saturating H121*. It is clear that after 0.4 s the effect on U has reached almost its full value while less than 50% of the limiting effect on U* has been attained. Since spin–lattice relaxation is unlikely to occur at very different rates in the two unfolded forms, this clearly demonstrates that folding to N from the minor unfolded component U occurs much more rapidly than from U*. The larger absolute magnitude of the MT effect ultimately observed for U* is simply because it constitutes much the greater proportion of the unfolded population.

Kinetics of Conformational Interconversions. The magnitudes of the MT effects observed in single and double saturation experiments were analyzed in order to determine the rates of the various interconversion processes. The method depends on modification of the Bloch equation governing the longitudinal magnetization according to the chemical exchange processes taking place (Forsen & Hoffman, 1963; Campbell et al., 1978). The conventional two-site formulation was extended to the present multisite system as outlined below.

On the basis of the qualitative results described above, the following kinetic scheme was set up:

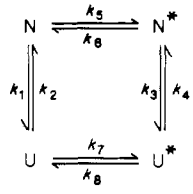

Possible direct interconversion of N and U* or N* and U was neglected in the present analysis. This point is discussed later. A further simplifying assumption was that the spin–lattice relaxation times (T_1) of the nuclei studied were equal, at 49 °C, to those measured outside the transition zone, where exchange effects were negligible. This permitted rate constants to be deduced directly from the limiting MT effects observed at 49 °C, obviating the necessity for time-dependent MT experiments, which would have been prohibitively demanding of protein and spectrometer time. Thus, spin–lattice relaxation times were measured by selective inversion recovery for H121 and H121* at 37 and 42 °C and found to be insensitive to the temperature change, thereby giving confidence in the validity of these values under the conditions of the MT experiments at 49 °C. Similarly, spin–lattice relaxation of the His $H^{\epsilon 1}$ resonances of unfolded nuclease at 53 °C appeared to be homogeneous, within experimental error, so that a value for T_1 was obtained from the selective inversion recovery of the cluster of resonances, and this value was used in analyzing the MT data.

The strategy for measuring the individual rate constants was as follows: Consider the case of H121. Its longitudinal magnetization, which we may denote N, is determined by a Bloch equation modified by the effects of the exchange processes shown in the kinetic scheme

$$\frac{dN}{dt} = \frac{N\{0\} - N}{T_{1,N}} - (k_1 + k_5)N + k_6N^* + k_2U \quad (1)$$

where $N\{0\}$ represents the unperturbed magnetization of H121, N^* the magnetization of H121*, and U that of the His-121 resonance of the U state. When a perturbation is applied that affects one or more terms on the right-hand side, N will in turn be affected and will tend to a limiting value given by the equilibrium condition $dN/dt = 0$.

In the double saturation experiment where both H121* and U,U* are saturated, the last two terms on the right in eq 1 vanish and the resulting magnetization of H121 has a limiting value, which we may denote $N\{UU^*,N^*\}$, given by

$$\frac{N\{0\} - N\{UU^*,N^*\}}{T_{1,N}} - (k_1 + k_5)N\{UU^*,N^*\} = 0 \quad (2)$$

Since we assume $T_{1,N}$ to be known, measurement of the MT effects thus permits solution for $(k_1 + k_5)$.

Similarly, when H121 and U,U* are simultaneously saturated, the magnetization of H121* will tend to a limiting value, $N^*\{UU^*,N\}$, given by

$$\frac{N^*\{0\} - N^*\{UU^*,N\}}{T_{1,N^*}} - (k_3 + k_6)N^*\{UU^*,N\} = 0 \quad (3)$$

whence $(k_3 + k_6)$ may be determined. When U,U* only are saturated, the effect on N is given by

$$\frac{N\{0\} - N\{UU^*\}}{T_{1,N}} - (k_1 + k_5)N\{UU^*\} + k_6N^*\{UU^*\} = 0 \quad (4)$$

Combining this with eq 2, we obtain

$$(N\{UU^*\} - N\{UU^*,N^*\})(1/T_{1,N} + k_1 + k_5) = k_6N^*\{UU^*\} \quad (5)$$

The value of $(k_1 + k_5)$ having been determined through eq 4, this result permits k_6 and, by substitution into eq 3, k_3 to be calculated.

In the same way, comparison of the single and double saturation effects on H121* gives

$$(N^*\{UU^*\} - N^*\{UU^*,N\})(1/T_{1,N^*} + k_3 + k_6) = k_5N\{UU^*\} \quad (6)$$

from which k_5 and in turn k_1 may be calculated.

These three experiments thus permit four rate constants to be determined, solely from intensity changes of H121 and H121* that were measurable directly in the spectrum. In order to obtain the other rates, experiments in which U and U* are not saturated were necessary. Since the uncertainty in the

Table II: Properties of Resonances Observed in MT Experiments

resonance	intensity at 49 °C[a]	spin–lattice relaxation time (s)
H121	$N\{0\} = 100 \pm 1$	$T_{1,N} = 0.63 \pm 0.04$[b]
H121*	$N^*\{0\} = 20 \pm 1$	$T_{1,N^*} = 0.55 \pm 0.08$[b]
U*	$U^*\{0\} = 171 \pm 16$	$T_{1,U} = 1.0 \pm 0.1$[c]
U	$N\{0\} = 9 \pm 7$	

[a] In arbitrary units. [b] Measured at 42 °C. [c] Measured for the envelope of His $H^{\epsilon 1}$ peaks of unfolded nuclease, 53 °C.

intensities, particularly of U, was substantially greater than that of the resonances of N and N*, particular care was necessary in deciding on the approach likely to yield the most reliable results in these cases.

When H121 alone is saturated, the effect on N^* is given by

$$\frac{N^*\{0\} - N^*\{N\}}{T_{1,N^*}} - (k_3 + k_6)N^*\{N\} + k_4U^*\{N\} = 0 \quad (7)$$

Comparison with eq 3 yields

$$(N^*\{N\} - N^*\{UU^*,N\})(1/T_{1,N^*} + k_3 + k_6) = k_4U^*\{N\} \quad (8)$$

From this result, k_4 may be determined. By analogy it is in principle possible to solve for k_2 according to

$$(N\{N^*\} - N\{UU^*,N^*\})(1/T_{1,N} + k_1 + k_5) = k_2U\{N^*\} \quad (9)$$

However, the extreme uncertainty in the value of $U\{N^*\}$ results, in practice, in very large error limits.

In order to calculate the rates of interconversion of U and U*, the strategy adopted was to compare the effects of saturating H121* alone with H121 and H121* together:

$$\frac{U^*\{0\} - U^*\{N^*\}}{T_{1,U}} - (k_4 + k_8)U^*\{N^*\} + k_7U\{N^*\} = 0 \quad (10)$$

$$\frac{U^*\{0\} - U^*\{N,N^*\}}{T_{1,U}} - (k_4 + k_8)U^*\{N,N^*\} + k_7U\{N,N\} = 0 \quad (11)$$

Combining these results leads to

$$\frac{U\{N^*\} - U\{N,N^*\}}{U^*\{N^*\} - U^*\{N,N^*\}} - \frac{k_8}{k_7} = \frac{k_4 + 1/T_{1,U}}{k_7} \quad (12)$$

Now, k_8/k_7 is just equal to the relative populations of U and U*, as required by the principle of detailed balance (Moore, 1972). Although this value is rather uncertain, it is a small number and therefore does not add significantly to the error limits. Taking this value from the simulation, it is then possible to solve eq 12 for k_7. The advantage of this formulation was that the only other experimental datum required was a ratio that was directly measurable from a difference spectrum; the absolute magnitudes of U^* and U, which carry relatively large uncertainty limits, were not explicitly required.

The series of MT experiments required for this analysis was performed at 49 °C, pH 5.3, just about the midpoint of thermal unfolding. The relative populations of the different states, as manifest in the intensities of the His-121 $H^{\epsilon 1}$ resonances, under those conditions are summarized in Table II, together with the T_1 values employed in the data analysis. The details of the MT effects and the calculated rate constants are presented in Table III. Two rate constants, k_2 and k_8, were not directly measured because unacceptable uncertainty accumulated in all convenient approaches to their calculation. These rates may be determined, however, by invoking the principle of detailed balance, which requires that for each individual pair of exchanging species the ratio of interconversion rate constants is equal to the ratio of populations. Thus, in terms of the spectral intensities, $N\{0\}/U\{0\} = k_2/k_1$; $U^*\{0\}/U\{0\} = k_7/k_8$. We may note that for those pairs of rate constants where independent determinations were possible, excellent conformity with this principle was obtained: $k_5/k_6 \simeq 5.0$ compares with $N\{0\}/N^*\{0\} = 5.0 \pm 0.5$; $k_3/k_4 \simeq 9.5$, again entirely consistent with the equilibrium $U^*\{0\}/N^*\{0\} = 8.5 \pm 1.4$. This gives us considerable confidence in the validity of the analysis. The rate constants (k/s^{-1}) that have been determined are summarized in the scheme below (numbers in parentheses indicate lower and upper limits of experimental uncertainty).

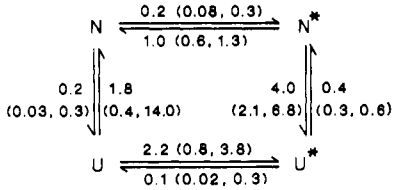

Discussion

Structural Model. The existence of alternative, slowly interconverting unfolded states of proteins is now firmly linked with cis/trans isomerism about X–proline peptide bonds (Brandts et al., 1975; Kim & Baldwin, 1982; Lin & Brandts, 1984; Schmid et al., 1986). Our MT studies of staphylococcal nuclease have revealed such a heterogeneity of the unfolded population, and kinetic measurements, detailed in this paper, suggest that this is structurally related to the observed heterogeneity of the folded population. This strongly suggests, therefore, that one of the six prolines of nuclease is in different orientations in the alternative folded froms N and N*.

The particular sensitivity of His-121 to the heterogeneities of both folded and unfolded populations suggested that Pro-117, which is closest in sequence and in the folded structure to His-121, was likely to be the specific residue involved. This

Table III: Quantitative Analysis of Magnetization-Transfer Experiments at 49 °C

resonances saturated	intensity changes[a]	analysis[b]	results (s^{-1})	result no.
U*, U, N	$N^*\{0\} - N^*\{UU^*,N\} = 15 \pm 1$	3	$k_3 + k_6 = 4.94 \pm 1.49$	i
U*, U, N*	$N\{0\} - N\{UU^*,N^*\} = 18 \pm 1$	2	$k_1 + k_5 = 0.34 \pm 0.04$	ii
U*, U	$N^*\{UU^*\} - N^*\{UU^*,N\} = 2 \pm 1$	6, i	$k_5 = 0.18 \pm 0.10$	iii
	$N\{UU^*\} - N\{UU^*,N^*\} = 4 \pm 1$	5, ii	$k_6 = 0.97 \pm 0.36$	iv
		ii, iii	$k_1 = 0.16 \pm 0.13$	v
		i, iv	$k_3 = 3.97 \pm 1.85$	vi
N	$U^*\{0\} - U^*\{N\} = 9 \pm 2$			
	$N^*\{N\} - N^*\{UU^*,N\} = 10 \pm 1$	8, i	$k_4 = 0.42 \pm 0.17$	vii
N*/N, N*	$[U^*\{N^*\} - U^*\{N,N^*\}]/[U\{N^*\} - U\{N,N^*\}] = 0.7 \pm 0.2$	11, vii	$k_7 = 2.2 \pm 1.6$	viii

[a] Values in arbitrary units, relative to unperturbed values given in Table II. [b] Equations 1–11 are as given in the text, prerequisite results denoted as in last column in this table.

was further supported on consideration of the crystal structure of the inhibited protein in relation to our data, as discussed below. In view of this evidence we then sought to test our model through a protein-engineering experiment (Evans et al., 1987). Substitution of glycine for proline at position 117 resulted in a protein whose NMR spectrum revealed overall folding similar to that of the wild type but contained no evidence for slowly interconverting folded forms. This was just the result expected from our model since glycine would be much less amenable than proline to the existence of alternative peptide bond orientations of comparable stability (Ramachandran & Mitra, 1976). MT studies of this mutant revealed no evidence for alternative unfolded forms comparable to those detected for the wild type either. This is particularly convincing evidence in support of our model, since in the absence of a cooperatively folded structure the effects of the sequence change are likely to be rather short range. Thus, the weight of evidence strongly supports a model in which the N and U forms of the nuclease contain Pro-117 in one orientation, while in N* and U* it is in the other orientation. We may thus proceed to consider the results presented in this paper in terms of this model.

Pro-117 has been observed to be in the cis orientation in the crystal structure of a nuclease–Ca^{2+}–nucleotide complex (Arnone et al., 1978; Cotton et al., 1979; T. R. Hynes and R. O. Fox, unpublished results). The NMR spectra showed that titration with the nucleotide led to progressive loss of the minor (N*) component, so that in the ternary complex the protein structure is N-like, in the context of this equilibrium. It is thus concluded that the N state contains the 116–117 peptide bond in a cis orientation, while in N* it is trans.

The magnetization transfer results show that N interconverts readily with U but slowly with U*, while N* interconverts rapidly with U*. Hence, it is concluded that U is the *cis*-proline form in the unfolded state and U* the trans form. The results show that U* is the predominant unfolded component. This is consistent with predictions from small peptide studies, which have shown that the trans isomer is usually the major one in the absence of folding interactions (Brandts et al., 1975; Grathwohl & Wüthrich, 1976).

In the crystal structure of the nuclease–Ca^{2+}–nucleotide inhibitor complex, Pro-117 is located in a type VI reverse turn (Richardson, 1981). *cis*-Proline at the third position is a requirement for this turn conformation, so rearrangement of the neighboring residues will be inevitable in the N* structure, where this proline is trans. However, it is evidently not sufficient to discuss the disparity between N and N* solely in terms of these localized effects, since the sensitivity of a considerable number of residues, including at least three of four histidines, indicates that small changes are propagated throughout much of the structure. This emphasizes the highly cooperative nature of the forces that determine the folding of the protein. This is further indicated by the selection of the N-like structure that results on inhibitor binding. While no direct interaction between residues 116 or 117 and the nucleotide is observed in the crystal structure, the side chain of the preceding Tyr-115 has been shown to undergo a large change of environment when the inhibitor complex is formed (Tucker et al., 1979b). Such a change could be a significant factor contributing to the observed change in the relative stabilities of the alternative turn conformations.

The relatively long-range conformational consequences of proline isomerization in the folded protein may be compared with similarly widespread effects that have been observed to result from single residue substitutions in nuclease (Hibler et al., 1987). In the Pro-117 → Gly mutant there were evidently small conformational differences from the wild-type structures, as evidenced by chemical shift changes of some resonances in the NMR spectrum (Evans et al., 1987). A detailed crystallographic study of this behavior is in progress (T. R. Hynes and R. O. Fox, unpublished results).

Table IV: Thermodynamics of Proline Isomerism in Folded and Unfolded Nuclease

$U_1 \rightarrow U_2$	$\Delta G^a = +8.8 \pm 2.3$ kJ mol^{-1}
	$\Delta H^b \approx 0$
	$\rightarrow \Delta S^c \approx -27 \pm 7$ J K^{-1} mol^{-1}
N* → N	$\Delta G^a = -4.3 \pm 0.3$ kJ mol^{-1}
	$\Delta H^a = -45 \pm$ kJ mol^{-1}
	$\rightarrow \Delta S^c = -126 \pm 17$ J K^{-1} mol^{-1}
	$\Delta G_{conf}{}^d = -13.1 \pm 2.6$ kJ mol^{-1}
	$\Delta H_{conf}{}^d \approx -45 \pm 5$ kJ mol^{-1}
	$\Delta S_{conf}{}^d \approx -99 \pm 24$ J K^{-1} mol^{-1}

[a] Determined experimentally in this work. [b] Estimated from model compound data (Brandts et al., 1975). [c] Deduced from the relation $\Delta G = \Delta H - T\Delta S$. [d] Conformational contributions, estimated as described in the text.

Thermodynamics of Folding and Proline Isomerism. From the relative intensities of their resonances, the free energy of U may be determined to be 8.8 ± 2.3 kJ mol^{-1} higher than that of U* at 49 °C. If it is assumed that it is attributable specifically to the difference between the alternative peptide bond orientations, this term must contribute toward the free energy difference between N and N*. Experimentally, N was determined to be lower in free energy by −4.3 ± 0.3 kJ mol^{-1} under these conditions. The discrepancy between these terms, amounting to some 13.1 ± 2.6 kJ mol^{-1} in favor of N, may then be identified with more favorable interactions arising from the overall fold of the protein when the *cis*- rather than *trans*-proline is accommodated.

The separate enthalpy and entropy contributions to these free energies may be analyzed in a similar way. The results are outlined below and summarized in Table IV. From the temperature dependence of their equilibrium constant, the enthalpy of N was found to be around 45 kJ mol^{-1} lower than that of N*. The enthalpy difference between U and U* was not measurable directly, since the U/U* ratio could not be determined with sufficient accuracy over a range of temperature. In order to proceed, it is therefore necessary to assume a value for this parameter. In small peptides, this value is generally close to zero (Brandts et al., 1975) and in the case of at least one protein in its unfolded state a value of zero has been deduced from kinetic measurements (Garel & Baldwin, 1975; Schmid & Baldwin, 1978). We therefore have made the assumption that this is also true for unfolded nuclease, in which case the enthalpy difference between N and N* can be seen to arise almost entirely from the wider conformational differences associated with the isomerism.

Using this assumption the entropy difference, calculated according to $\Delta S = (\Delta H - \Delta G)/T$, is around −27 ± 7 J K^{-1} mol^{-1} for U* → N compared to −126 ± 17 J K^{-1} mol^{-1} for N* → N. Thus, N* has the higher entropy of the two folded states and, once again, the discrepancy cannot be accounted for solely by the local difference of peptide bond orientation. Rather, the higher entropy of N* may indicate that the globular structure, or a significant segment of it, is less rigid than that of N. In support of this we may note that the chemical shifts of the N* resonances are generally closer to random coil values than those of N, suggesting increased dynamic averaging of interresidue interactions with the N* structure.

It should be noted that this analysis assumes that contributions from differences in solvation to the free energy difference between *cis*- and *trans*-proline isomers in the unfolded state are also present in the folded states. Even with this reservation, however, the general conclusions are clear: In spite of an entropy difference that favors the *trans*-proline form, N*, the equilibrium in the folded state is driven over so that N is the predominant form, as a result of a large enthalpy term that can be ascribed to more favorable bonding interactions within the overall N conformation.

Kinetics of Folding and Isomerization. In the quantitative kinetic analysis it was assumed that N and U* could interconvert only via N* or U. Similarly, N* and U were assumed not to interconvert directly. In terms of the model this amounts to saying that the peptide bond isomerization and main-chain folding events must be sequential rather than simultaneous. This may be seen to be a reasonable assumption since the absence of detectable intermediates implies that both processes are rare but intrinsically fast. Thus, the probability of, for example, isomerization occurring in a partially folded molecule would be very slight, owing to the extremely fleeting existence of such species. This argument would break down only if the mechanism of folding were such that the barrier to isomerization was dramatically lowered as a result of distortions at some intermediate stage. There is no evidence for such an effect.

According to our model both the U* $\rightleftharpoons$ U and N* $\rightleftharpoons$ N interconversion processes are proline isomerization events with, in the latter case, accompanying minor rearrangements of the folded structure. For an Ala–Pro peptide bond in a small peptide, isomerization rates of 0.02 s^{-1} (trans $\rightarrow$ cis) and 0.2 s^{-1} (cis $\rightarrow$ trans) have been determined at this temperature (Grathwohl & Wüthrich, 1981). These are somewhat slower than the U* $\rightleftharpoons$ U rates measured here, with a relaxation time $(k_{cis \rightarrow trans} + k_{trans \rightarrow cis})^{-1}$ of between 0.3 and 1.2 s for the unfolded protein compared to 4.5 s for the model compound. However, it has been established that the nature of the preceding residue can have a large effect on these rates (Grathwohl & Wüthrich, 1981) so that it will be necessary to study a peptide containing a Lys–Pro bond, as in the nuclease, before any conclusions can be drawn as to the signficance of this disparity.

In the folded state the relative populations are very different, so it is difficult to compare rate constants, but the relaxation time for N $\rightleftharpoons$ N* is around 0.8 s, which is comparable to that for U* $\rightleftharpoons$ U. This suggests that interaction with other residues in the folded structures has little influence on the barrier to proline isomerization. Studies of the temperature dependence of the N $\rightleftharpoons$ N* interconversion kinetics that should shed further light on this behavior are in progress. It would be of interest to compared the case of ribonuclease A where the trans $\rightarrow$ cis isomerization of a proline occurs significantly faster in a metastable intermediate than in the unfolded state (Schmid, 1986). In that case the rate of the reverse reaction is not known, so it is not possible to assess the similarity of that behavior to that observed in nuclease.

The processes N $\rightleftharpoons$ U and N* $\rightleftharpoons$ U* are folding/unfolding transitions in which the 116–117 peptide bond orientation is conserved, though those of the other prolines may not be. It should be noted that although we have assumed that U and U* are kinetically homogeneous, this has not been experimentally verified, and there could, in reality, be further subpopulations that, though not spectroscopically distinguished, fold at different rates. On the assumption, however, that folding is rigorously a two-state equilibrium, simple curves such as those shown in Figure 6 may be used to approximate the free energy profile of the folding/unfolding processes (Go & Abe, 1981). Clearly, a key question in protein folding regards the nature of the activated state in such a profile. Although such a state is perhaps unlikely to be structurally unique (Harrison & Durbin, 1985), it has been possible to draw some general conclusions in the light of kinetic data (Kim & Baldwin, 1982; Goldenberg & Creighton, 1985). In the present case we may address, in particular, the issue of the stabilization of the cis peptide bond relative to the trans through folding interactions. If the specific interactions that achieve this stabilization were effective at an early stage of folding, before the rate-determining steps, then it would be anticipated that folding U $\rightarrow$ N would be greatly accelerated compared to U* $\rightarrow$ N*, while unfolding of N and N* would be predicted to occur at similar rates. This is illustrated in Figure 6a. On the other hand, if the *cis*-proline turn became stabilized only at a late stage, subsequent to the rate-limiting events, the folding rates would be expected to be similar, while N* would be much the more rapid to unfold (Figure 6b). A further possibility would be that both folding and unfolding were facilitated by one or other Pro-117 orientation, as a result of differences in pathways or interactions in the activated state. Such a case is illustrated in Figure 6c.

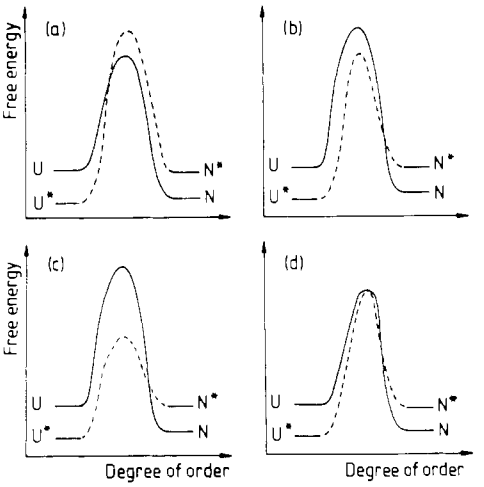

FIGURE 6: Schematic free energy profiles for the folding and unfolding processes of staphylococcal nuclease having a cis (solid line) or trans (dashed line) oriented peptide bond preceding Pro-117. The four sketches illustrate possible limiting cases, as discussed in the text.

The experimental data may then be examined in the light of these considerations. The situation of Figure 6a can immediately be ruled out, since unfolding of N* is in fact much faster than that of N. This means that the activated state is not native-like in its discrimination between cis and trans orientations at Pro-117. The folding rates are not known with such precision as the unfolding rates, but still it is clear that folding of N* is not significantly faster than that of N, in contrast to its unfolding. This rules out a situation such as that of Figure 6c: there is no evidence that the folding pathways of the *cis*- and *trans*-proline forms are very different other than in the immediate consequences of peptide bond orientation. Given the experimental uncertainties, it is not possible to be certain whether the limiting case of Figure 6b pertains or whether there is an intermediate situation as illustrated in Figure 6d. Broadly, however, it may be asserted that the *cis*-proline turn conformation is fully stabilized only at a late stage in the folding process. It has been proposed that the activated state in folding may in general be a highly strained conformation close to the native structure (Creighton & Goldenberg, 1985). The present results would indicate that

in the case of nuclease the distortions present in the activated state impinge upon the turn formed by residues 115–118, seriously diminishing the specific stabilization it affords to the cis peptide bond in the N state.

The major folded and unfolded states are N and U*, respectively, in which Pro-117 is in different orientations. The MT results have shown that their interconversion could occur at significant rates by at least two quite distinct pathways, with peptide bond isomerization either preceeding or following the main-chain folding events. The significance of these alternative routes was evaluated by computer simulation of the transfer of labeled U* molecules to N via N* or U, according to the rate constants determined in the MT studies. It was found that between 8% and 60% of molecules passed through N as an intermediate, the remainder through N*, confirming that both pathways are significant. This conclusion strongly supports the contention that it is necessary to consider any specific pathway as one of many possibilities for the folding of a protein (Harrison & Durbin, 1985).

The significance of proline isomerism in protein folding has been the subject of considerable interest (Brandts et al., 1975; Kim & Baldwin, 1982) and continues to be a controversial issue (Lin & Brandts, 1984; Schmid et al., 1986). In this paper we have established a clear relationship between the isomerism about a specific X–Pro peptide bond and the folding of staphylococcal nuclease. It has been shown that Pro-117 can exist in alternative orientations in both folded and unfolded forms of the protein and that wider conformational differences between the alternative structured forms have significant consequences for the thermodynamics of folding. In spite of the complexity of the system it has been possible not only to elucidate the kinetic interelationships of the different states of the protein but also to determine rates for most of the interconversion processes at equilibrium and to use these to draw conclusions about the nature of the folding process.

Registry No. Staphylococcal nuclease, 9013-53-0; L-proline, 147-85-3.

References

Alexandrescu, A. T., Mills, D. A., Ulrich, E. L., Chinami, M., & Markley, J. L. (1988) *Biochemistry 27*, 2158.

Anfinsen, C. B. (1973) *Science (Washington, D.C.) 181*, 223.

Arnone, A., Bier, C. J., Cotton, F. A., Day, V. W., Hazen, G. E., Richardson, D. C., Richardson, J. S., & Yonath, A. J. (1971) *J. Biol. Chem. 246*, 2302.

Boyd, J., Moore, G. R., & Williams, G. (1984) *J. Magn. Reson. 58*, 511.

Brandts, J. F., Halvorson, H. R., & Brennan, M. (1975) *Biochemistry 14*, 4953.

Campbell, I. D., Dobson, C. M., Ratcliffe, R. G., & Williams, R. J. P. (1978) *J. Magn. Reson. 29*, 397.

Cotton, F. A., Hazen, E. E., & Legg, M. J. (1979) *Proc. Natl. Acad. Sci. U.S.A. 76*, 2551.

Dobson, C. M., & Evans, P. A. (1984) *Biochemistry 23*, 4267.

Dobson, C. M., Evans, P. A., & Williamson, K. L. (1984) *FEBS Lett. 168*, 331.

Evans, P. A. (1986) D.Phil. Thesis, Oxford University.

Evans, P. A., Dobson, C. M., Hatfull, G., Kautz, R. A., & Fox, R. O. (1987) *Nature (London) 329*, 266.

Forsen, S., & Hoffman, R. A. (1963) *J. Chem. Phys. 39*, 2892.

Fox, R. O., Evans, P. A., & Dobson, C. M. (1986) *Nature (London) 320*, 6058.

Garel, J. R., & Baldwin, R. L. (1975) *J. Mol. Biol. 94*, 611.

Go, N., & Abe, H. (1981) *Biopolymers 20*, 991.

Goldenberg, D. P., & Creighton, T. E. (1985) *Biopolymers 24*, 167.

Grathwohl, C., & Wüthrich, K. (1976) *Biopolymers 15*, 2025.

Grathwohl, C., & Wüthrich, K. (1981) *Biopolymers 20*, 2623.

Harrison, S. C., & Durbin, R. (1985) *Proc. Natl. Acad. Sci. U.S.A. 82*, 4028.

Hibler, D. W., Stolowich, N. J., Reynolds, M. A., Gerlt, J. A., Wilde, J. A., & Bolton, P. H. (1987) *Biochemistry 26*, 6278.

Jeener, J., Meier, B. H., Bachmann, P., & Ernst, R. R. (1979) *J. Chem. Phys. 71*, 4546.

Kim, P. S., & Baldwin, R. L. (1982) *Annu. Rev. Biochem. 51*, 549.

Lin, L. N., & Brandts, J. F. (1984) *Biochemistry 23*, 5713.

Maniatis, T., Fritsch, E. F., & Sambrook, J. (1982) *Molecular Cloning—A Laboratory Manual*, Cold Spring Harbor Laboratory, Cold Spring Harbor, NY.

Marion, D., & Wüthrich, K. (1983) *Biochem. Biophys. Res. Commun. 113*, 967.

Markley, J. L., & Jardetzky, O. (1970) *J. Mol. Biol. 50*, 223.

Moore, W. J. (1972) *Physical Chemistry*, 5th ed., p 341, Longmans, London.

Morris, G. A., & Freeman, R. (1978) *J. Magn. Reson. 29*, 433.

Ramachandran, G. N., & Mitra, A. K. (1976) *J. Mol. Biol. 107*, 85.

Richardson, J. S. (1981) *Adv. Protein Chem. 29*, 433.

Rosenberg, M., Ho, Y., & Shatzman, A. (1093) *Methods Enzymol. 101*, 123.

Schmid, F. X. (1986) *FEBS Letts. 198*, 217.

Schmid, F. X., & Baldwin, R. L. (1978) *Proc. Natl. Acad. Sci. U.S.A. 75*, 4764.

Schmid, F. X., Grafl, J. R., Wrba, A., & Beintema, J. J. (1986) *Proc. Natl. Acad. Sci. U.S.A. 83*, 872.

Shortle, D. (1986) *J. Cell. Biochem. 30*, 281.

Tucker, P. W., Hazen, E. E., & Cotton, F. A. (1979a) *Mol. Cell. Biochem. 23*, 3.

Tucker, P. W., Hazen, E. E., & Cotton, F. A. (1979b) *Mol. Cell. Biochem. 23*, 121.